Nonlinear optical properties of a Pöschl-Teller quantum well

Hasan Yıldırım and Mehmet Tomak*
Department of Physics, Middle East Technical University, Ankara 06531, Turkey
(Received 6 May 2005; revised manuscript received 7 July 2005; published 28 September 2005)

The nonlinear optical properties of quantum wells (QWs) represented by a Pöschl-Teller confining potential are studied. This potential is well suited for such purposes as it can easily become asymmetrical by a correct choice of its parameter set. We calculate the linear and the third-order nonlinear optical intersubband absorption coefficients, the second-harmonic generation (SHG) susceptibility tensor, and optical rectification (OR) under the density matrix formalism. Numerical results for a typical GaAs QW are presented. The resulting SHG and the OR coefficients are much larger than their values for bulk GaAs.

DOI: 10.1103/PhysRevB.72.115340 PACS number(s): 78.67.De, 42.65.Ky

I. INTRODUCTION

The nonlinear optical properties of quantum wells (QWs) and other low-dimensional systems have attracted an enormous interest in recent years.[1–25] Especially second-order nonlinear optical properties,[10–19] such as second-harmonic generation (SHG), optical rectification (OR), and electro-optic effect (EOE), and third-order optical properties,[1–9,20–22] such as third-order absorption, and third-harmonic generation are extensively studied. This is because these nonlinearities have the potential for device applications in far-infrared laser amplifiers,[23] photodetectors,[24] and high-speed electro-optical modulators.[25]

The linear intersubband absorption within the conduction band of a GaAs QW has been studied experimentally with[4] and without[5,6] an electric field. A very large dipole strength and a narrow band width have been observed, which suggest that the intersubband optical transition in QWs may have huge nonlinearities. On the theoretical side, Ahn and Chuang studied linear and nonlinear intersubband absorptions in QWs with[1,3] and without[2] an electric field. Yuen[7] and Shi and Pan[8] studied a semiconductor superlattice. Zhang[9] considered electric-field-biased semiparabolic QWs. Results reveal that the linear and nonlinear intersubband absorptions significantly depend on the structure of the system and the applied electric field.

The second-order susceptibility is negligible except for the small contribution of the bulk susceptibility in symmetric QWs.[11] However, when the inversion symmetry of the system is broken, it is possible to obtain a significant second-order susceptibility.[11–13] Asymmetric QWs can be created in two ways: either by advanced material growing technology[13–15] or by an external applied electric field.[10,11,16] Gurnick and DeTemple[14] obtained an asymmetric QW by growing $Al_xGa_{1-x}As$ multiple QWs with asymmetric composition gradients of Al in the growth direction and calculated the second-order nonlinearities for a Morse potential. They obtained 10−100 times larger values than those of bulk materials. Yuh and Wang[15] investigated a step QW, and Rosencher and Bois[13] have shown that the QWs could be designed so that the absorption could be doubly resonant and the SHG susceptibility could be more than 1000 times higher than that in bulk GaAs. Khurgin[12] proposed an asymmetric coupled QW. Fejer *et al.*[16] observed an order of magnitude larger second-order susceptibility than that in the bulk case in GaAs QWs with an electric field. Guo and Gu[17] studied OR and EOE in a parabolic QW with an applied electric field. Results reveal a significant enhancement of both properties with the increasing electric field. They obtained one and six orders of magnitude higher values for OR and EOE than those in the bulk GaAs, respectively. Also, Zhang and Xie[18,19] calculated EOE and the SHG susceptibility and they found about two orders of magnitude larger EOE than that in the parabolic QW with an applied electric field.

In this work, QWs having the Pöschl-Teller potential[26] are considered. This potential has not been studied extensively in the literature and to the best of our knowledge only Radovanovic *et al.*[27] used the modified Pöschl-Teller potential to calculate intersubband absorption based on bound-bound, bound-free, and free-free transitions in QWs.

The Pöschl-Teller potential has tunable asymmetry degree and the corresponding Schrödinger equation is analytically solvable.[28] The tunable asymmetry of the potential, therefore, is expected to yield promising nonlinear optical properties. The results show that with the increasing asymmetry parameter the total absorption peak increases and the peak position has an obvious blueshift. The relative distance between peak positions of the SHG coefficient gets larger while both have a blueshift with the increasing asymmetry parameter. We obtain large SHG and OR coefficients.

The organization of this paper is as follows. In Sec. II, the exact wave functions and eigenenergies are given and the expressions for linear and nonlinear absorption coefficients, SHG and OR, are derived under the density matrix formalism. In Sec. III, numerical implementation on typical GaAs material is presented. A brief conclusion is given in Sec. IV.

II. THEORY

The effective-mass Hamiltonian for the electrons in a potential well, $V(z)$ is

$$H = -\frac{\hbar^2}{2m^*}\left[\frac{\partial^2}{\partial x^2} + \frac{\partial^2}{\partial y^2} + \frac{\partial^2}{\partial z^2}\right] + V(z), \tag{1}$$

where

$$V(z) = \frac{\hbar^2\beta^2}{2m^*}\left[\frac{\kappa(\kappa-1)}{\sin^2(\beta z)} + \frac{\eta(\eta-1)}{\cos^2(\beta z)}\right],$$

$$\kappa, \eta > 1 \tag{2}$$

Here z represents the growth direction. The Pöschl-Teller potential[26,28] $V(z)$ is governed by three parameters: κ, η, and β. This potential has singularities at $z=0$ and at $z=\pi/2\beta$. The parameters κ and η tune the degree of the asymmetry, and the potential profile is perfectly symmetric for $\kappa=\eta$.

The eigenfunctions $\psi_{n,k}(\mathbf{r})$ and eigenenergies $\varepsilon_{n,k}$, are given, respectively, by

$$\psi_{n,k}(\mathbf{r}) = \phi_n(z)\exp(i\mathbf{k}_\parallel \cdot \mathbf{r}_\parallel), \tag{3}$$

$$\varepsilon_{n,k} = E_n + \frac{\hbar^2}{2m^*}|\mathbf{k}_\parallel|^2, \tag{4}$$

where $\mathbf{k}_\parallel$ and $\mathbf{r}_\parallel$ are the wave and position vectors in the xy plane. $\phi_n(z)$ and E_n are the envelope wave function and transverse energy of the nth subband, respectively, and are the solutions of the Schrödinger equation

$$H_z\phi_n(z) = E_n\phi_n(z), \tag{5}$$

where H_z is the z component of the Hamiltonian H. $\phi_n(z)$ and E_n are given by[28]

$$\phi_n(z) = C_N \sin^\kappa(\beta z)\cos^\eta(\beta z) \times {}_2F_1\left(-n, \kappa+\eta+n, \kappa+\frac{1}{2}; \sin^2(\beta z)\right), \tag{6}$$

$$E_n = \frac{\hbar^2\beta^2}{2m^*}(\kappa+\eta+2n)^2 n = 0,1,2,\ldots. \tag{7}$$

Here C_N is the normalization constant.

We consider an optical radiation of angular frequency ω applied to the system with the polarization along the growth direction z. The incident field can be written as

$$E(t) = \mathrm{Re}(E^0 e^{-i\omega t}) = Ee^{-i\omega t} + E^* e^{i\omega t}. \tag{8}$$

The one-electron density matrix equation with intraband relaxation is

$$\frac{\partial\rho_{ij}}{\partial t} = \frac{1}{i\hbar}[H_0 - qzE(t), \rho]_{ij} - \Gamma_{ij}(\rho-\rho^{(0)})_{ij}, \tag{9}$$

where H_0 is unperturbed Hamiltonian. The Γ_{ij} elements are taken to be equal to one value Γ_0 only. Equation (9) is solved via the iterative method,[29,30] by noting that

$$\rho(t) = \sum_n \rho^{(n)}(t), \tag{10}$$

with

$$\frac{\partial\rho_{ij}^{(n+1)}}{\partial t} = \frac{1}{i\hbar}[H_0, \rho^{(n+1)}]_{ij} - \Gamma_0\rho_{ij}^{(n+1)} - \frac{1}{i\hbar}[qz, \rho^{(n)}]_{ij}E(t). \tag{11}$$

The electronic polarization $P(t)$ and the susceptibility $\chi(t)$ caused by the optical field $E(t)$ can be expressed through the dipole operator μ and the density matrix as[29,30]

$$P(t) = \chi(\omega)Ee^{-i\omega t} + \chi(-\omega)E^* e^{i\omega t} = \frac{1}{V}\mathrm{Tr}(\rho\mu), \tag{12}$$

where V is the volume of the system and Tr stands for the trace.

The absorption coefficient and the susceptibility are related by[31]

$$\alpha(\omega) = \frac{4\pi\omega}{n_r c}\,\mathrm{Im}[\chi(\omega)], \tag{13}$$

where n_r is the refractive index of the system and the c is the speed of the light. By using the density matrix formalism and the iterative procedure,[3,29,30] the linear and the third-order absorption coefficients, $\alpha^{(1)}(\omega)$ and $\alpha^{(3)}(\omega)$, are derived for both symmetric and asymmetric potentials. We neglect the higher-harmonic terms and consider only the steady-state response. The first-order and third-order absorption coefficients are found to be

$$\alpha^{(1)}(\omega) = \frac{4\pi\omega}{n_r c}\frac{\sigma_s|\mu_{10}|^2\hbar\Gamma_0}{(E_{10}-\hbar\omega)^2 + (\hbar\Gamma_0)^2}, \tag{14}$$

$$\alpha^{(3)}(\omega) = -2\omega\left(\frac{4\pi}{n_r c}\right)^2 \frac{I\sigma_s|\mu_{10}|^4\hbar\Gamma_0}{((E_{10}-\hbar\omega)^2 + (\hbar\Gamma_0)^2)^2} \times\left(1 - \frac{|\mu_{11}-\mu_{00}|^2}{4|\mu_{01}|^2} \frac{\times\{(E_{10}-\hbar\omega)^2 - (\hbar\Gamma_0)^2 + 2E_{10}(E_{10}-\hbar\omega)\}}{E_{10}^2 + (\hbar\Gamma_0)^2}\right). \tag{15}$$

Here I is the intensity of the incident field, σ_s is the density of the electrons, $E_{10}=E_1-E_0$, and μ_{ij} is the matrix element of the dipole operator $\mu_{ij}=\langle\phi_i|qz|\phi_j\rangle(i,j=0,1)$. $\alpha^{(1)}(\omega)$ keeps its form, whether the potential is symmetric or not. However, the second term in Eq. (15) is zero when the potential is symmetric. We write the total absorption coefficient $\alpha(\omega,I)$ as

$$\alpha(\omega,I) = \alpha^{(1)}(\omega) + \alpha^{(3)}(\omega,I). \tag{16}$$

Derivation of the second-harmonic generation requires the consideration of the higher-order terms,[10] such as $(e^{\pm 2i\omega t})$. We get the SHG which is observable only in the case of asymmetric potentials as

$$\chi_{2\omega}^{(2)} = \frac{\sigma_s|\mu_{10}|^2(\mu_{11}-\mu_{00})}{(2\hbar\omega - E_{10} + i\hbar\Gamma_0)(\hbar\omega - E_{10} + i\hbar\Gamma_0)}, \tag{17}$$

where only the near-resonant term at $2\hbar\omega \cong E_{10}$ is considered.

The coefficient of the constant term which contributes zero frequency in the SHG expression is the OR coefficient and it is given by[13,17,19]

$$\chi_0^{(2)} = 8\frac{\sigma_s|\mu_{10}|^2(\mu_{11}-\mu_{00})E_{10}^2}{[(\hbar\omega - E_{10})^2 + (\hbar\Gamma_0)^2][(\hbar\omega + E_{10})^2 + (\hbar\Gamma_0)^2]}. \tag{18}$$

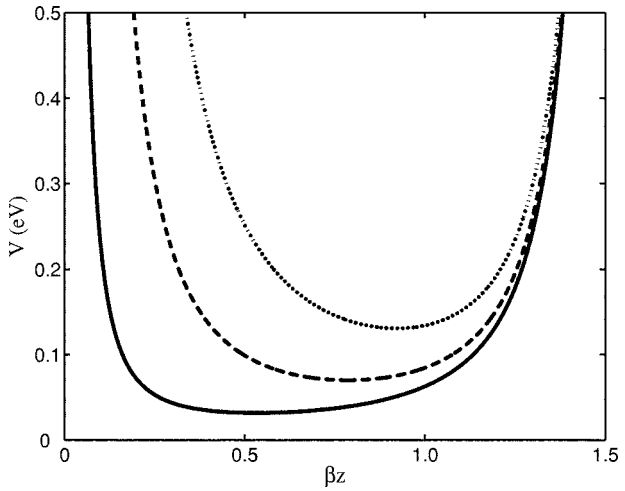

FIG. 1. The Pöschl-Teller potential profiles for $\eta=2$. The solid curve stands for $\kappa=1.2$, the dashed curve for $\kappa=2$, and the dotted curve for $\kappa=3$.

III. NUMERICAL RESULTS AND DISCUSSION

We use the following input parameters:[3] $\sigma_s=3\times10^{16}$ cm^{-3}, $\Gamma_0=1/0.14$ ps^{-1}, $n_r=3.2$, $m^*=0.067m_0$. The length of the quantum well, L, and β are taken to be 126.5 Å and $\pi/2L$, respectively.

In Fig. 1, the potential profile is shown for three different κ values, i.e., $\kappa=1.2$, $\kappa=2$, and $\kappa=3$, while η equals to 2. For $\kappa=\eta$, the curve becomes symmetric around $\beta z=\pi/4$, for $\kappa>\eta$ it becomes oblique and its minimum is shifted to the right. However, for $\kappa<\eta$ minimum of the curve is shifted to the left.

The first three normalized wave functions for the same κ and η values are shown in Fig. 2(a)–2(c). It can be observed that the shapes of the wave functions are very similar to the shapes of the wave functions of the parabolic potential with and without the electric field.[18] This is due to the behavior of the potential around its minimum value where it may approximately be replaced by a parabolic curve.[28]

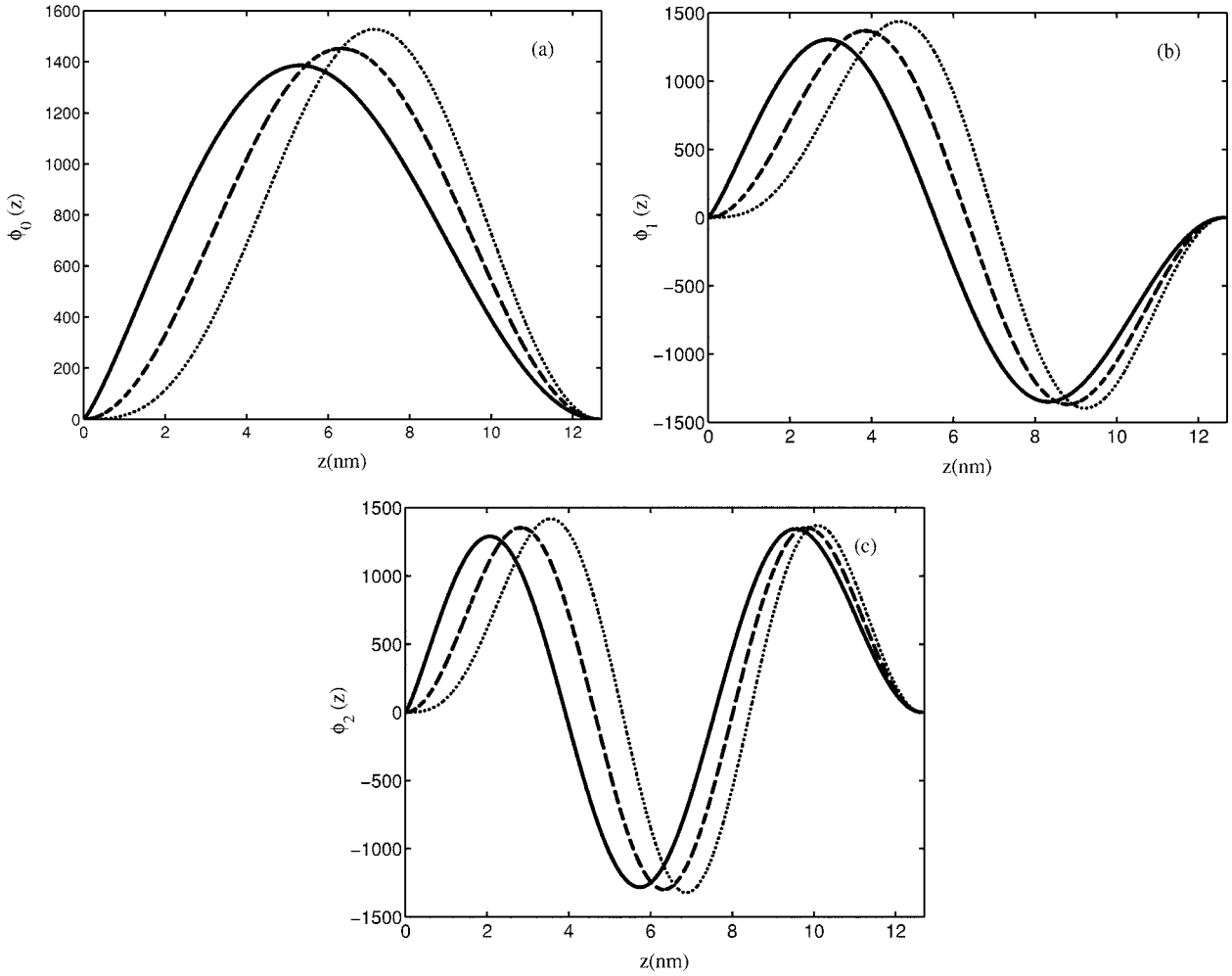

FIG. 2. The normalized first three wave functions of the QW having the Pöschl-Teller confining potential. The solid curves stand for $\kappa=1.2$, the dashed curves for $\kappa=2$, and the dotted curves for $\kappa=3$ in panels (a), (b), and (c).

TABLE I. The calculated energy eigenvalues for the first three eigenfunctions in eV for $\eta=2$.

κ	E_0	E_1	E_2
1.2	0.0897	0.2369	0.4541
1.4	0.1013	0.2554	0.4797
1.6	0.1135	0.2747	0.5060
1.8	0.1265	0.2947	0.5330
2.0	0.1402	0.3154	0.5606
2.2	0.1545	0.3367	0.5890
2.4	0.1696	0.3588	0.6181
2.6	0.1854	0.3816	0.6479
2.8	0.2018	0.4051	0.6784
3.0	0.2190	0.4292	0.7096

We list the first three energy eigenvalues for κ between 1.2 and 3 in Table I. In the table, we observe that the energy levels are not equally spaced. This can be explained by the quadratic form of eigenenergies [Eq. (7)] where the difference between two successive energy levels is

$$\Delta E_{n+1,n} = \frac{2\hbar^2\beta^2}{m^*}(\kappa+\eta+2n+1). \tag{19}$$

The linear absorption coefficient $\alpha(\omega, I=0)=\alpha^{(1)}(\omega)$ and the total absorption coefficient $\alpha(\omega, I)$ as functions of the incident photon energy at $I=1.0$ MW/cm^2 are shown in Fig. 3. The peak position of the linear absorption coefficient has a blueshift with increasing κ, because the energy difference between first-excited and ground states has a linear dependency on the κ. However, the peak value does not grow but remains almost constant. The resonant peak value (i.e., $\hbar\omega = E_{10}$) of the linear absorption coefficient is proportional to $E_{10}|\mu_{10}|^2$. Our calculations show that this product is more or less constant when $1.2 \leqslant \kappa \leqslant 3$ and $1.2 \leqslant \eta \leqslant 2$. The total absorption coefficient in Fig. 3 increases with increasing κ. The resonant peak value of the total absorption coefficient is shown as a function of κ and η in Fig. 4. We see that the higher the η the higher the peak value. The Eq. (15) is totally negative at resonance and it is proportional to

$$E_{10}|\mu_{10}|^2\left(|\mu_{10}|^2 + \frac{|\mu_{11}-\mu_{00}|^2(\hbar\Gamma_0)^2}{4E_{10}^3}\right). \tag{20}$$

The first term in the parentheses decreases with increasing κ and η. This is because as asymmetry parameters increase, the potential well becomes narrower yielding smaller $|\mu_{10}|^2$. Although the symmetry is broken for $\kappa \neq \eta$ and $|\mu_{11}-\mu_{00}|^2$ increases, the second term in Eq. (20) becomes smaller since it is inversely proportional to E_{10}^3. $\alpha^{(3)}(\omega)$ decreases in magnitude and as a result the resonant peak value of the total absorption coefficient increases.

The SHG coefficient as a function of incident photon energy for the asymmetric Pöschl-Teller potential is shown in Fig. 5. In the figure, the solid line stands for $\kappa=1.2$ and the dotted line for $\kappa=3$. The curve for $\kappa=3$ is multiplied by three for clarity. The increasing κ value yields reduction in both peaks up to $\kappa=2$ for which the SHG is zero, but for $\kappa>2$ the SHG peaks have nonzero values although smaller than the peaks for $\kappa<2$. The peak positions have an obvious blueshift while their separation increases. These can be attributed to the linear κ dependence of the energy difference between two successive levels as in Eq. (19). The maximum value for the SHG coefficient is about 15 times larger than the one in bulk[32] GaAs for $\kappa=1.1$. However, when the other input parameters quoted in the literature[13,16] are used, it is possible to obtain larger peak values. For example, if the density of the electrons is increased up to the order of 10^{17} cm^{-3} the SHG peak increases more than two orders of magnitude. The electrons are, apart from thermal generation, supplied by dopant atoms. However, this supply is limited by the solubility of the dopant atom in GaAs.[13] At higher-electron densities, a good description of the optical properties of QWs must take

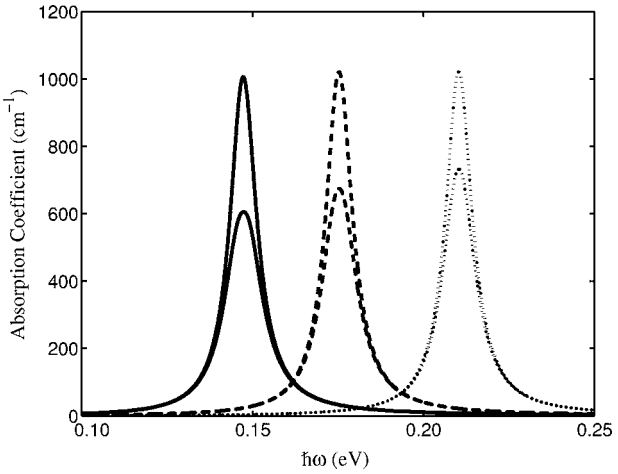

FIG. 3. The linear and the total absorption coefficients as a function of photon energy for the optical intensity $I=1.0$ MW/cm^2 and for $\eta=2$. The solid curve stands for $\kappa=1.2$, the dashed curve for $\kappa=2$, and the dotted curve for $\kappa=3$,

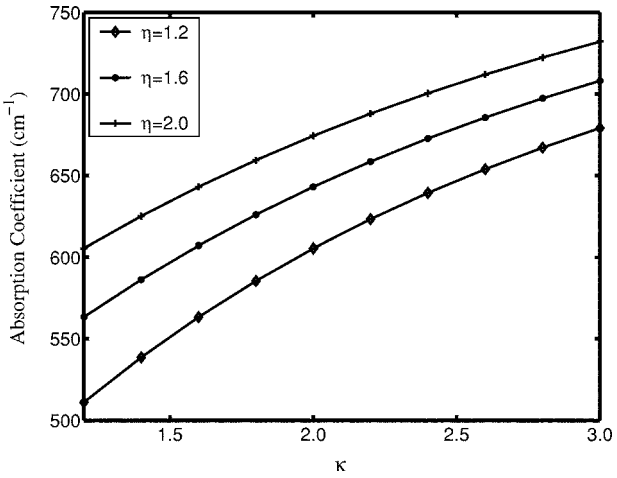

FIG. 4. The resonant peak value of the total absorption coefficient as a function of the parameter κ for various η values. $I=1.0$ MW/cm^2.

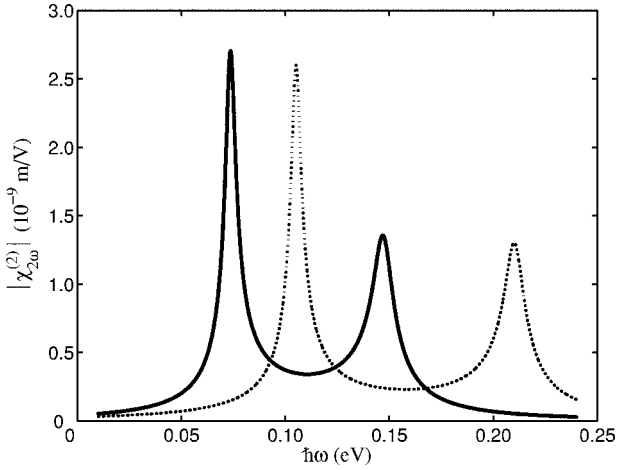

FIG. 5. The SHG coefficient $|\chi^{(2)}_{2\omega}|$ as a function of photon energy for $\eta=2$. The solid curve stands for $\kappa=1.2$ and the dotted curve for $\kappa=3$ (multiplied by three for a better view).

into account the interactions among those electrons. The peak value of the SHG tensor at $2\hbar\omega=E_{10}$ is displayed in Fig. 6 as a function of κ and η. The SHG is zero at $\kappa=\eta$. The peak increases with $|\mu_{11}-\mu_{00}|$ as the asymmetry is introduced. But the E_{10}^2 in the denominator substantially reduces the peak value at higher values of the asymmetry parameters.

We also calculate the OR coefficient for the κ values of 1.2 and 3.0. The results are shown in Fig. 7. The peaks have a blueshift with increasing κ. The peak value of the solid line corresponds to three orders of magnitude larger values than in bulk[32] GaAs. However, this number can be enhanced when the other electron densities and relaxation times are used as mentioned above. For example, with the σ_s of the order of 10^{17} cm^{-3} and $1/\Gamma_0$ of 0.2 ps^{-1}, for $\kappa=1.1$, we get four orders of magnitude larger values than in bulk GaAs. The relaxation time, however, is certainly governed by intrinsic mechanisms such as electron-electron scattering, impurity scattering, collisions among electrons, optical-phonon emission for an excitation energy higher than 36 meV, well inhomogeneities, and temperature of the system.[3,13,18] In Fig. 8, the peak value of the OR coefficient at resonance frequency, i.e., $\hbar\omega=E_{10}$, is showed. The peak exhibits the similar pattern with the peak value of the SHG coefficient, except that it is reduced with E_{10}.

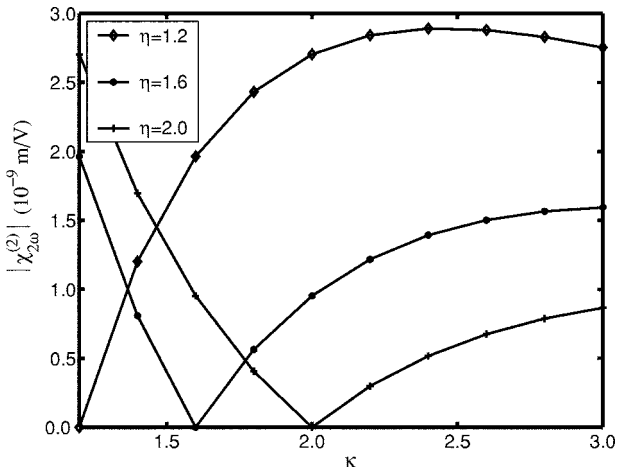

FIG. 6. The resonant peak value of the SHG coefficient as a function of the parameter κ for various η values.

FIG. 7. The OR coefficient $|\chi^{(2)}_{0}|$ as a function of photon energy for $\eta=2$. The solid curve stands for $\kappa=1.2$ and the dotted curve for $\kappa=3$.

IV. CONCLUSION

The nonlinear optical properties of QWs described by a Pöschl-Teller confining potential are studied. We have calculated the linear and third-order absorption coefficients, the second-order susceptibility, and the optical rectification for symmetric and asymmetric cases of the Pöschl-Teller potential under the density matrix formalism. We find that the total absorption is reduced by nearly 30% and this reduction decreases with increasing asymmetry parameters at $I=1.0$ MW/cm^2. We calculate SHG and OR coefficients much larger than in the bulk GaAs. The peak positions

FIG. 8. The resonant peak value of the OR coefficient as a function of the parameter κ for various η values.

strictly depend on the asymmetry parameter. Our investigation of the peak value of the SHG and OR coefficients for various κ and η show that a feasible SHG or OR coefficient is possible only for κ and $\eta < 2$. The QWs represented by the Pöschl-Teller confining potential seem to be possible with the recent progresses in the nanofabrication technology. An electric-field-biased QW having a Pöschl-Teller type confining potential is expected to yield a larger SHG.

*Corresponding author. Electronic address: tomak@metu.edu.tr

[1] D. Ahn and S. L. Chuang, Phys. Rev. B **35**, R4149 (1987).
[2] D. Ahn and S. L. Chuang, J. Appl. Phys. **62**, 3052 (1987).
[3] D. Ahn and S. L. Chuang, IEEE J. Quantum Electron. **QE-23**, 2169 (1987).
[4] A. Harwitt and J. S. Harris Jr., Appl. Phys. Lett. **50**, 685 (1987).
[5] B. F. Levine *et al.*, Appl. Phys. Lett. **50**, 273 (1987).
[6] L. C. West and S. J. Eglash, Appl. Phys. Lett. **46**, 1156 (1985).
[7] S. Y. Yuen, Appl. Phys. Lett. **43**, 813 (1983).
[8] J. J. Shi and S. H. Pan, Superlattices Microstruct. **17**, 91 (1995).
[9] L. Zhang, Opt. Quantum Electron. **36**, 665 (2004).
[10] L. Tsang, D. Ahn, and S. L. Chuang, Appl. Phys. Lett. **52**, 697 (1988).
[11] L. Tsang, S. L. Chuang, and S. M. Lee, Phys. Rev. B **41**, 5942 (1990).
[12] J. Khurgin, Phys. Rev. B **38**, 4056 (1988).
[13] E. Rosencher and P. Bois, Phys. Rev. B **44**, 11315 (1991).
[14] M. K. Gurnick and T. A. DeTemple, IEEE J. Quantum Electron. **QE-19**, 791 (1983).
[15] P. F. Yuh and K. L. Wang, J. Appl. Phys. **65**, 4377 (1989).
[16] M. M. Fejer, S. J. B. Yoo, R. L. Byer, A. Harwit, and J. S. Harris, Phys. Rev. Lett. **62**, 1041 (1989).
[17] K. X. Guo and S. W. Gu, Phys. Rev. B **47**, 16322 (1993).
[18] L. Zhang and H. J. Xie, Phys. Rev. B **68**, 235315 (2003).
[19] L. Zhang and H. J. Xie, Mod. Phys. Lett. B **17**, 347 (2003).
[20] G. H. Wang, Q. Guo, and K. X. Guo, Phys. Status Solidi B **238**, 75 (2003).
[21] L. Zhang and H. J. Xie, Physica E (Amsterdam) **22**, 791 (2004).
[22] K. X. Guo and C. Y. Chen, Physica B **262**, 74 (1999).
[23] R. F. Kazarinov and R. A. Suris, Sov. Phys. Semicond. **5**, 707 (1971).
[24] F. Capasso, K. Mohammed, and A. Y. Cho, IEEE J. Quantum Electron. **QE-22**, 1853 (1986).
[25] D. A. B. F. Miller, Int. J. High Speed Electron. Syst. **1**, 19 (1991).
[26] G. Poschl and E. Teller, Z. Phys. **83**, 143 (1933).
[27] J. Radovanovic, V. Milanavic, Z. Ikonic, and D. Indjin, Phys. Lett. A **269**, 179 (2000).
[28] S. Flugge, *Practical Quantum Mechanics I* (Springer-Verlag, Berlin, 1971).
[29] R. W. Boyd, *Nonlinear Optics* (Academic Press, San Diego, 2003).
[30] N. Bloembergen, *Nonlinear Optics* (World Scientific, Singapore, 1996).
[31] H. Haug, *Quantum Theory of the Optical and Electronic Properties of Semiconductors* (World Scientific, Singapore, 1994).
[32] A. Yariv, *Quantum Electronics* (John Wiley, New York, 1989).